Aperiodic stochastic resonance with correlated noise

A. Capurro,[1,2,*] K. Pakdaman,[1] T. Nomura,[1] and S. Sato[1]
[1]*Department of Systems and Human Science, Division of Biophysical Engineering, Graduate School of Engineering Science, Osaka University, Toyonaka, 560-8531 Osaka, Japan*
[2]*Neurophysiology Department, Institute of Biological Research Clemente Estable, Avenida Italia 3318, Montevideo 11600, Uruguay*
(Received 27 May 1998)

We examine the influence of the noise correlation on aperiodic stochastic resonance. To this end, we compute the discharge rate of a FitzHugh-Nagumo neuron model in response to a slow sub-threshold aperiodic input in the presence of additive correlated noise. Aperiodic stochastic resonance is observed for each level of noise correlation; i.e., there exists a noise amplitude that maximizes the covariance between the input signal and the model's discharge rate. Both the maximal covariance and the optimal noise level depend on the noise correlation. The former remains almost constant for low noise correlations, and steadily decreases at larger correlations. The latter displays a U-shaped curve when plotted against the noise correlation, indicating that aperiodic stochastic resonance occurs at lower noise amplitudes for an appropriate range of noise correlation. We show that the results are consistent with the evaluation of the discharge rate of the model through a quasistatic assumption. Our results suggest that the interplay of the noise correlation with the time scales of the neuron model can lead to an improvement of the aperiodic stochastic resonance effect, in that for an appropriate level of correlation maximal covariance can be attained with lower noise amplitude.
[S1063-651X(98)08010-5]

PACS number(s): 87.10.+e, 87.22.Jb, 05.40.+j

I. INTRODUCTION

In general, the presence of internal or external noise disturbs signal processing and transmission in natural and artificial systems. However, there are instances where the noise can have a beneficial effect. For example, it has been shown that noise of appropriate amplitude can linearize the input output relation in sensory neurons receiving suprathreshold periodic stimulation by reducing nonlinear distortions in the output (for a review see [1]), or allow the detection of weak subthreshold periodic signals through stochastic resonance (SR) [2]. These phenomena have also been analyzed theoretically in order to better determine the conditions under which they may actually occur in nervous systems [3,4]. The aforementioned studies focus mainly on the response of systems to sine-like periodic signals. Of equal importance has been the investigation of the influence of noise on the response of sensory neurons and neuronal models to aperiodic signals. In this respect, it has been shown that the presence of noise can also enhance the transmission of weak aperiodic input signals. More precisely, the covariance or the correlation between the input signal and the discharge rate of the system are maximized at an intermediate noise level [5]. This phenomenon referred to as aperiodic stochastic resonance (ASR) has been observed in experimental preparations [6] as well as in various neuronal models [7]. From the theoretical standpoint, ASR has been studied, under the quasistatic assumption, for slowly varying input signals [8], as well as through the linear response theory for weak input signals [9]. The former established a link between ASR and noise-induced linearization (e.g., [1]), while the latter related it to conventional SR.

The aforementioned studies on ASR mainly concentrate on the influence of noise amplitude on the response of the system. The purpose of the present work is to assess the importance of another noise characteristic, namely, the noise correlation time, on ASR. This point is motivated by the fact that the noise used in the previous studies is usually quasi-white, i.e., it displays short correlation times. While this assumption is justified from a theoretical standpoint, and also in many practical applications, natural systems are often subject to correlated noise, with a wide range of possible correlation times.

Similar considerations have been at the basis of the study of the influence of noise correlation on conventional SR. In weakly periodically modulated bistable systems with a double well potential, SR is well characterized by the fact that the noise-induced interwell switchings occur mostly at the modulation period (for reviews see [10,11]). Taking into account noise correlation introduces a third time scale into the system, which directly affects the rate of interwell hopping, thereby modifying the conditions for SR. It has been shown in fact that at a given noise amplitude, the interwell switching rate decreases with the noise correlation, so that the more correlated the noise is and the higher the noise amplitudes that are required to reach SR [11]. Moreover, measures such as spectral amplification and output signal-to-noise ratio that are maximized at SR display lower peaks for larger noise correlations. Therefore, in such systems, noise correlation reduces the beneficial effects of SR by requiring larger noise amplitudes to attain lower optimal performances.

In this work, we examine the effect of noise correlation time on ASR displayed by the FitzHugh-Nagumo (FHN) neuron model subject to a weak aperiodic stimulation and

*Electronic address: alberto@bpe.es.osaka-u.ac.jp

additive correlated noise. We show that the effect of noise correlation on ASR can differ from the one described in the previous paragraph, in that the system can perform better at intermediate correlation times than at shorter or longer ones.

This paper is organized as follows. In Sec. II, we describe the neuron model. Section III is devoted to the presentation of the results. Finally a discussion is presented in Sec. IV.

II. THE NEURON MODEL

In this section, we describe the dynamics of the neuron model and methods used for the computation of the various quantities needed to assess the effect of noise correlation on ASR. We closely follow the methods in [8]. We describe consecutively the FHN model, the noise and the signal characteristics, the spike detection scheme, and the method used to obtain an estimation of the signal from the model's output spike train.

a. The FHN model. The dynamics of the FHN model receiving an input signal $S(t)$, and a noise $n(t)$ is described by the following system of differential equations:

$$\varepsilon\frac{dv}{dt}=v(v-a)(1-v)-w+A+S(t)+n(t),$$
$$\frac{dw}{dt}=v-w-b, \tag{2.1}$$

where v represents the membrane potential of the model and w is the recovery variable. Throughout our study, we used the parameters $\varepsilon=0.005$, $a=0.5$, $b=0.15$, and $A=0.04$, as in [8]. We integrated system (2.1) using a forward Euler algorithm with a fixed step-size of 0.001 time units.

b. The noise $n(t)$. We used both white Gaussian and correlated noise in our study. The latter was modeled as an Ornstein-Uhlenbeck (OU) stochastic process satisfying

$$\frac{dn}{dt}=-\lambda_1 n+\lambda_2\xi, \tag{2.2}$$

where ξ is white Gaussian noise with autocorrelation $\langle\xi(t)\xi(t')\rangle=\delta(t-t')$. The OU process solution of Eq. (2.2) is a zero-mean Gaussian process with autocorrelation:

$$\langle n(t)n(t')\rangle=\frac{\lambda_2^2}{2\lambda_1}\exp(-\lambda_1|t-t'|). \tag{2.3}$$

In order to investigate the effect of the noise correlation time $\tau=1/\lambda_1$, we used the following values: $\lambda_1=500.0$, 250.0, 100.0, 50.0, 20.0, 10.0, 5.0, 3.0, 2.0, 1.0 and 0.1. A good approximation to white noise can be produced using $\lambda_1=1/$ (step size), but for this case we used white Gaussian noise directly.

In the abscissa of Fig. 3 and Fig. 5 (*C* and *D*) the noise correlation time $\tau=1/\lambda_1$ was represented using a logarithmic transformation as the ''level of correlation of the noise'' C_L

$$C_L=3-\log_{10}(\lambda_1). \tag{2.4}$$

This transformation gives $C_L=0$ for a noise with $\lambda=1000$ (i.e., white noise when using an integration step size of 0.001 time unit), and the value of C_L increases with the increase in the correlation time τ. Thus, C_L behaves as an appropriate measure of the level of correlation of the noise.

The standard deviation of the noise $n(t)$, denoted by σ, is given by $\sigma=\lambda_2/\sqrt{2\lambda_1}$, and depends on both λ_1 and λ_2. Therefore, when changing the correlation time of the noise $\tau=1/\lambda_1$, the value of λ_2 was adjusted accordingly to preserve the same value for σ. We checked that the shapes of the histograms of the noise obtained in this way were the same for the different correlation times.

c. The signal $S(t)$. The signal, denoted $S(t)$, was produced by passing the output of Eq. (2.2) (with $\lambda_1=0.05$ and $\lambda_2=0.05$) through a time-unit area Hanning window filter with 10 time units width. The standard deviation of $S(t)$ was set to 0.03, by multiplying the values of the time series by an appropriate factor. $S(t)$ has zero mean, lasts 250 time units, and is subthreshold, in the sense that it does not evoke any discharges in the absence of noise. Figure 1 shows the time course of the signal. The correlation time of this signal, i.e., 26.382 time units, is considerably larger than any relevant time scale of the dynamical system such as, for example, the duration of a spike ($\simeq 0.3$ time unit).

d. Spike detection scheme. The value of $v(t)$ reached at the peak of the spikes ranged from 1.0 to 1.1. A spike was detected when $v(t)$ exceeded a detection threshold set at 0.8. Furthermore, each spike detection was followed by a dead period of 0.4 time units during which further upward crossings of the detection threshold were not considered as new discharges [8].

e. Estimation of $S(t)$ *from the spike train.* A pulse of unit amplitude was assigned to each spike. In order to estimate the discharge rate $R(t)$ of the model, the pulse train was convolved with a three time unit half-width Hanning window.

Two measures were then used to evaluate the input-output fidelity of the model. These were the covariance (C_0) and (normalized) correlation (C_1) between $S(t)$ and $R(t)$ and were calculated according to [12]:

$$C_0=\overline{[S(t)-\overline{S(t)}][R(t)-\overline{R(t)}]}, \tag{2.5}$$

$$C_1=\frac{C_0}{\overline{[[S(t)-\overline{S(t)}]^2[R(t)-\overline{R(t)}]^2]^{1/2}}}. \tag{2.6}$$

The general procedure and values of the parameters follows [8], with the remarkable difference that the amplitude of the input signal is bigger. This change increases the peak values of C_1 from 0.30 to 0.8, implying that the matching in shape between $S(t)$ and $R(t)$ is better. The peak value of C_0 decreases, because in the computation of the latter quantity the relative size of the signals to be compared is also taken into account. Furthermore, the use of a signal with larger amplitude decreases the variability of both C_0 and C_1. Thus, the number of realizations of the model needed to obtain significant differences between the mean values of C_0 or C_1 for different levels of noise is drastically reduced.

III. RESULTS

In this section, we first describe how the ASR in the FHN is affected by the noise correlation time, and then through an

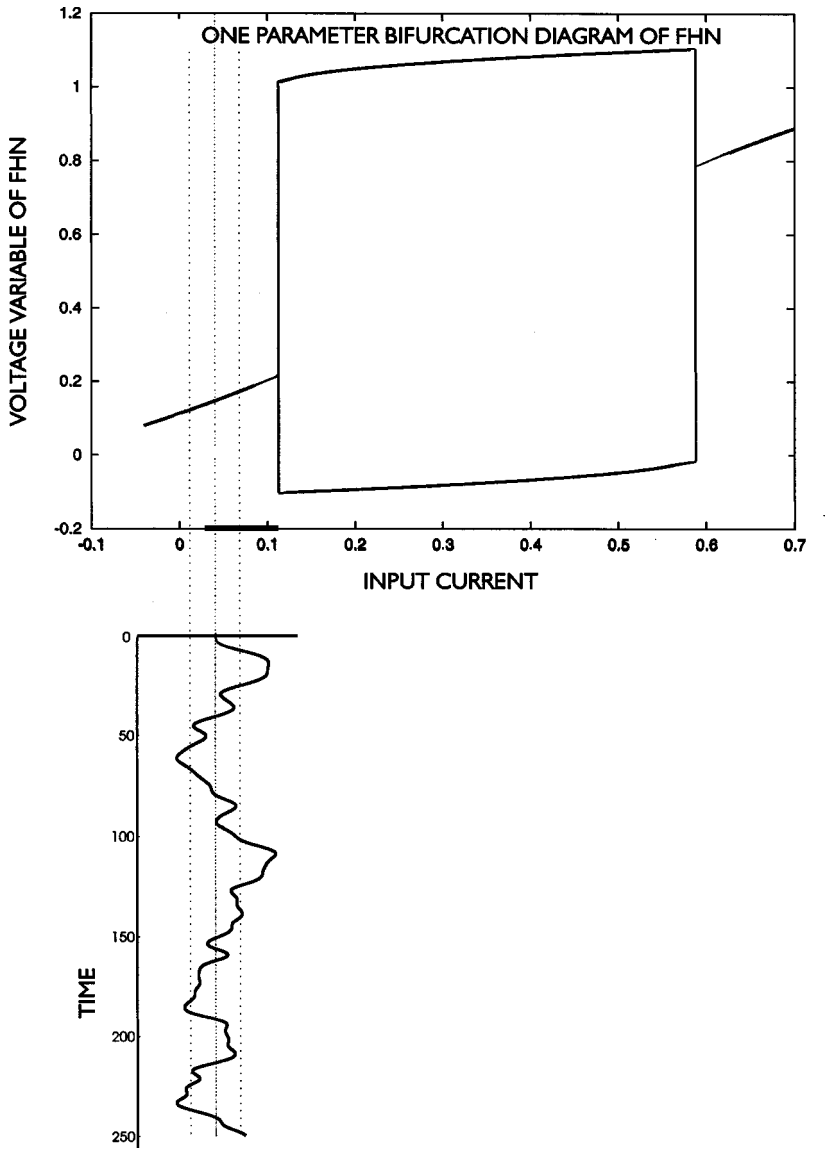

FIG. 1. Time series of the aperiodic subthreshold input signal $S(t)$ in the context of the one parameter bifurcation diagram of the FHN for the parameters used in the simulations. The one-parameter bifurcation diagram was calculated analytically before the first Hopf bifurcation and after the second Hopf bifurcation, and using a simulation in between both bifurcation points. The levels of A corresponding to the mean, and to the mean $\pm\sigma$ of the signal are indicated with dotted lines. The dark bar on the abscissa indicates the range of A where the system displays focus behavior. Abscissa: A in arbitrary units of current for the one-parameter bifurcation diagram, and time in arbitrary time units for the signal. Ordinate: v in arbitrary voltage units for the one parameter bifurcation diagram and A in arbitrary units of current for the signal.

evaluation of the discharge rate of the model under a quasistatic assumption, and a study of a simplified model, we provide an explanation for this phenomenon.

A. ASR in the FitzHugh-Nagumo neuron model with correlated noise

ASR takes place when the output discharge rate of the FHN best reproduces the input signal at some intermediate noise amplitude, with higher and lower noise levels deteriorating the input-output fidelity. ASR is characterized by the fact that, when plotted against the noise amplitude, the input-output covariance C_0 and normalized correlation C_1 are humpshaped.

Figure 2 shows C_1 (left column) and C_0 (right column) against the noise amplitude for the model described in the previous section, for three noise correlation times. Each curve displays ASR in that it has a maximum at some optimal noise amplitude σ^*. Thus, ASR is also present with correlated noise. Nevertheless, the two main features of ASR, that is the optimal noise amplitude that maximizes C_1 or C_0, and the values of these maxima, show a strong dependence on the noise correlation time.

The dependence of the optimal noise amplitude σ^* on the noise correlation time τ is as follows. Figure 2 shows that the mode of both C_1 and C_0 decreases when τ is increased up to some point $\tau^*=0.1$ time units (upper and middle rows), after which the mode increases with further increase in τ (bottom row). This can be seen in Fig. 3(a), which represents σ^* against the level of correlation of the noise C_L (2.4).

The resulting plot is U-shaped [Fig. 3(a)]. The minimum of the curve represents the level of correlation ($C_L=1.7$ to

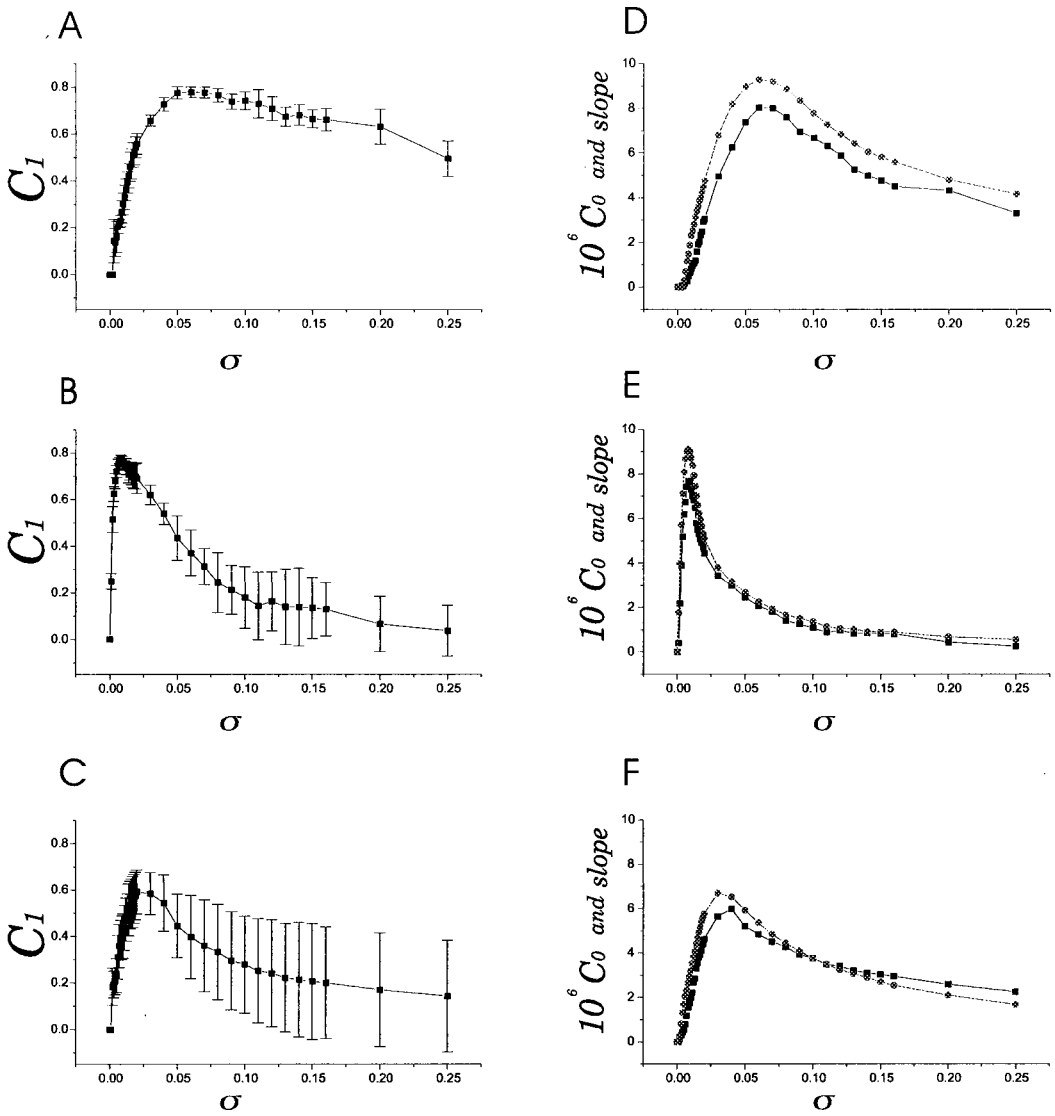

FIG. 2. The left column shows the ensemble averaged values of $C_1 \pm$ standard deviation for white noise (a), noise with correlation time $\tau=0.1$ (b), and noise with correlation time $\tau=10.0$ (c), plotted against the amplitude of the noise σ. The right column shows the ensemble-averaged values of $C_0\times 10^6$ (squares) and of the slope of the FHN input-output function (circles) for white noise (d), noise with correlation time $\tau=0.1$ (e), and noise with correlation time $\tau=10.0$ (f), plotted against the amplitude of the noise σ. All the points represent averages of 10 realizations of the model lasting 250 time units each, using a different seed of noise in each realization. Abscissa: σ in arbitrary units of current. Ordinate: C_1 (dimensionless) for the left column; $C_0\times 10^6$ in *current units* $\times$ (spikes/time units) (squares) and slope in spikes/(time units $\times$ current units) (circles) for the right column.

$C_L=2.3$, i.e., $\tau_a=0.5$ to $\tau_a=0.2$ time units) at which less noise is required to maximize C_0 and C_1. We also noted that the σ^* for C_0 coincides with the σ^* for C_1 in all cases with the only exception of the noise with the highest level of correlation ($C_L=4.0$, $\tau=10.0$). In this case $\sigma^*(C_0) > \sigma^*(C_1)$. The similar behavior of C_0 and C_1 (2.5 and 2.6) is expected, as the variance of the signal $S(t)$ is constant and the variance of the estimation of the signal $R(t)$ for σ^* does not change in a large extent for different correlations of the noise C_L (with the exception of the noise with higher level of correlation). Thus C_0 and C_1 are roughly proportional.

The dependence of the maximal input-output fidelity on the noise correlation time is somewhat different from that of σ^*. Figure 2 shows that the maximum value of C_1 and C_0 (reached at σ^*) is almost at the same level as for white noise for correlation time $\tau=0.1$ time units (upper and middle row, respectively). For larger correlation times, however, the maxima decrease (bottom row). This can be seen in Figs. 3(b) and 3(c), which show the maximal value of C_1 and C_0 against C_L. At low noise correlations, the curve displays a plateau, and then it monotonously decreases at larger correlation times. Interestingly, the value of τ^* is included in the plateau of this curve. Thus, the noise with $C_L=2.0$, i.e, $\tau=10.0$, minimizes σ^* without losing input-output fidelity.

In order to better understand the dependence of ASR on noise correlation, we apply the quasistatic approximation described in [8].

B. The quasistatic assumption

In the studies of ASR, in general, the input signal is relatively slow compared with the time scales of the neuron or the neuron model, such as spike and refractory period dura-

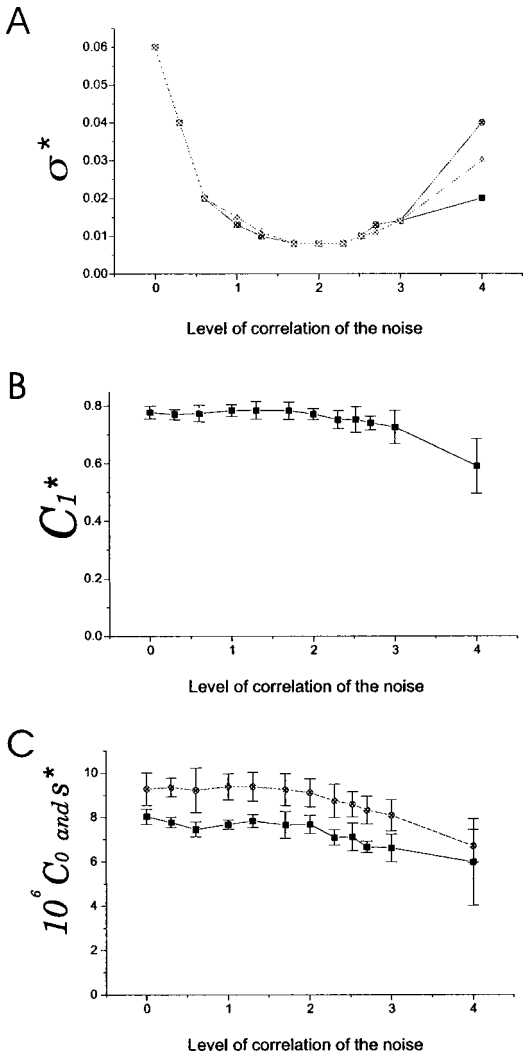

FIG. 3. (a) The σ^* for C_1 (squares), the σ^* for C_0 (circles), and the σ^* for the slope of the FHN input-output function (triangles) are plotted against the level of correlation of the noise C_L. (b) The maximum level of $C_1 \pm$ standard deviation, reached at σ^*, is plotted against C_L. (c) The maximum level of $C_0 \times 10^6 \pm$ standard deviation (squares) and the maximum slope of the FHN input-output function $\pm$ standard deviation (circles) reached at σ^*, are plotted against C_L. All the points represent averages of 10 realizations of the model lasting 250 time units each, using a different seed of noise in each realization. Abscissa: Level of correlation of the noise, C_L (dimensionless). Ordinate: σ^* in units of current for (a), C_1 at σ^* (dimensionless) for (b). For 3C, $C_0 \times 10^6$ at σ^* in current units$\times$(spikes/time units) (squares) and slope at σ^* in spikes/(time units$\times$current units) (circles).

tions. Chialvo *et al.* [8] took advantage of this, and showed that, under this condition, the system acts like a static nonlinearity. As the signal changes on a slower time scale than all characteristics times of the neuron, it produces quasistatic variations in the parameter A. Thus, the firing rate observed near a given value of the input signal can be estimated from the input-output function at the corresponding constant value of A. They determined the input-output function of this static system by computing the discharge rate of the model in response to constant current stimulation. Finally, they validated their approximation by showing numerically that the curve of C_0 against the noise level could be reproduced, up

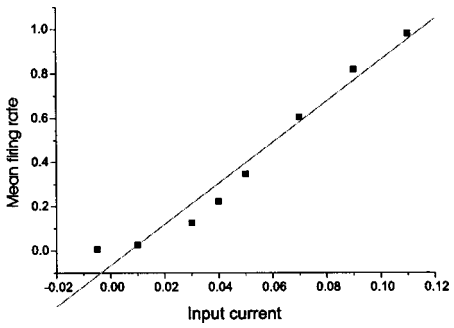

FIG. 4. The mean firing rate of the FHN is plotted against the input current A (squares). The 8 levels of A range from the minimum to the maximum of $S(t)$. The linear function fitted to the points by linear regression is shown with a dashed line. In this example $\sigma = 0.06$ and $C_L = 0.0$ (white noise), the value of the slope is 9.278 18, and the correlation coefficient between the squares and the dashed line is 0.981 78. Abscissa: A in arbitrary units of current. Ordinate: Mean firing rate in spikes/(time unit).

to a constant factor, by computing the slope of the mean firing rate $\overline{R(t)}$ as a function of tonic activation A for various noise intensities.

Chialvo *et al.* [8] performed their study with quasi white noise. Nevertheless, noise correlation does not significantly alter their results as long as the input signal is slow enough. We confirmed this point by computing numerically the static input-output function of the FHN in the presence of correlated noise of various intensities.

More precisely, we selected eight levels of constant current ranging from the minimum value to the maximum value of the signal $S(t)$. For each level of A we computed the mean firing rate of the FHN and obtained an input-output function for each value of σ. The mean firing rate was calculated as (number of spikes)/(simulation time) [13]. The slope of the input-output function was determined by linear regression. An example of this input-output function is shown in Fig. 4.

The slope was plotted against the noise amplitude σ. This plot matches, up to a constant factor, the plot of covariance against σ for all the levels of noise correlation tested [Fig. 2 (right column)]. The plot of the σ^* for the slope of the input output function versus C_L matches the plot of σ^* for C_0 versus C_L [Fig. 3(a)]. Also the plot of the slope at σ^* versus C_L matches up to a constant factor the plot of C_0 at σ^* versus C_L [Fig. 3(c)].

The above results show that the quasistatic assumption holds, and that in order to clarify the effect of noise correlation time on the ASR, we need only to compute the discharge rate of the model in response to constant input currents. Therefore, in the following, we examine how the discharge rate of a simplified version of the FHN varies with the noise correlation time, in order to determine the factors that are essential in obtaining a similar response.

C. Discharge rate of a simplified neuron model with correlated noise

In this section, we describe the influence of correlated noise on the response of a simplified FHN (SFHN) model. In other words, for each level of noise correlation C_L, we compute (i) the noise amplitude σ^* that maximizes the slope of

the constant current intensity versus mean firing rate curves, and (ii) the corresponding maximal slope value s^*. Next we monitor how these two quantities change with the noise correlation time.

The motivating reason for the construction of the SFHN was the schematic separation of the dynamics of the model into subthreshold and suprathreshold regimes. The latter represents the action potential whose shape and duration are little affected by the inputs. Therefore, we assumed that the response of the model was mainly shaped by the interaction between its intrinsic subthreshold dynamics and the noise. As a first approximation, we used the linearized FHN for the description of the subthreshold dynamics.

More precisely, the SFHN comprises two variables denoted by v' and w', and a constant threshold, denoted by θ. While v' is below threshold, the time course of the system is determined by the linearized FHN:

$$\varepsilon\frac{dv'}{dt}=\alpha(A)v'-w'+n(t),$$
$$\frac{dw'}{dt}=v'-w', \tag{3.1}$$

where $\alpha(A)=-3v^{*2}+2(a+1)v^*-a$, where v^* is the equilibrium potential for Eq. (2.1) for a constant current of intensity A. The noise n is determined by Eq. (2.2).

Concerning the threshold, it was necessary to define a level such that if the voltage of the SFHN exceeds its value the model is considered to fire. We took the difference v_H-v^*, where v_H is the equilibrium potential at the constant current intensity at which the Hopf bifurcation occurs, as this threshold value θ (see Fig. 1). We called v_H-v^* the threshold of the SFHN, in the sense that it plays the role of the threshold in the FHN, although in the latter system the threshold is not precisely defined as a single value.

In this way, for each value of the parameter A representing the constant current intensity, the subthreshold dynamics of the simplified model closely follow those of the FHN linearized at the equilibrium point. Furthermore, the threshold is adjusted to take into account that increasing A lowers the firing threshold in the FHN.

Whenever v' exceeds the threshold θ, both variables v' and w' are reset instantaneously to zero. This event constitutes the definition of the spike; the shape of the action potential itself is not explicitly included in this model. Following the post-discharge reset, the two variables v' and w' remain at the origin during an absolute refractory period lasting 0.4 time units, which is close to the duration of the spike in the FHN driven by noise (0.25–0.4 time units), and corresponds also to the dead time in the spike detection scheme used for the FHN. At the end of this period, the two variables evolve again according to Eq. (3.1).

In the numerical computations of the discharge rate of Eq. (3.1), we used exactly the same 8 values of the input amplitude A, and the same noise sequences that were used for the FHN. For the 6 larger values of A, the linearized FHN behaves as a focus; i.e., the eigenvalues of Eq. (3.1) are complex numbers. For the remaining two lower values of A the system behaves as a node. The region of focus behavior is indicated with a dark bar over the abscissa of Fig. 1. This

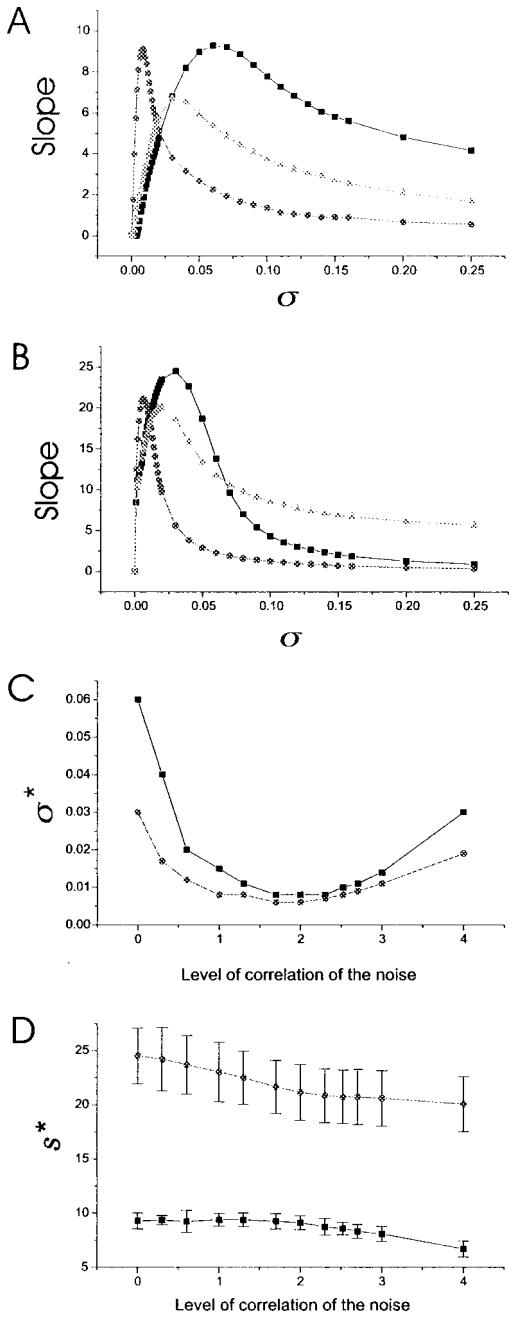

FIG. 5. (a) The slope of the FHN input-output function is plotted against the noise amplitude σ, for white noise (squares), noise with correlation time $\tau=0.1$ (circles), and noise with correlation time $\tau=10.0$ (triangles). (b) The slope of the SFHN input-output function is plotted against the noise amplitude σ, for white noise (squares), noise with correlation time $\tau=0.1$ (circles), and noise with correlation time $\tau=10.0$ (triangles). (c) The σ^* for the slope of the FHN input-output function (squares) and the σ^* for the slope of the SFHN input-output function (circles) are plotted against the level of correlation of the noise C_L. (d) The slope of the FHN input-output function $\pm$ standard deviation reached at σ^* (squares) and the slope of the SFHN input-output function reached at σ^* (circles) are plotted against C_L. All the points represent averages of 10 realizations of the model lasting 250 time units each, using a different seed of noise in each realization. Abscissa: σ in arbitrary current units for (a) and (b); level of correlation of the noise, C_L (dimensionless) for (c) and (d). Ordinate: Slope in spikes/(time units)$\times$(current units) for (a) and (b); σ^* in current units for (c) and slope at σ^* in spikes/(time units$\times$current units) for (d).

corresponds to a value of $\alpha(A) > -0.146\,421$ and to a value of the voltage variable $v > 0.136\,489$.

The slope of the input-output function versus σ for three different levels of noise correlation is shown in Fig. 5. The curves of the FHN system [Fig. 5(a)] and the SFHN [Fig. 5(b)] display a similar behavior. σ^*, the noise level that maximizes the slope, decreases with τ up to C^*, after which σ^* increases again. This phenomenon produces a U-shaped curve in the plot of σ^* versus C_L. The minimum of the curve is the same for both the FHN and the SFHN. In the latter, the U is ''flatter'' than in the former, i.e., the edges of the U have lower ordinates [Fig. 5(c)]. The maximum slope (s^*, the slope at σ^*) reaches larger values than in the FHN, and it decreases moderately as τ is increased. This trend to decrease is clearer than in the FHN, where there is a plateau that extends until $C_L = 2.0$ [Fig. 5(d)].

These simulations show that the performance of the SFHN is quite similar to that of the FHN, although the details are different. This implies that the properties of the FHN in the presence of noise can be studied using the SFHN as a plausible approximation. The behavior of the SFHN can be more easily investigated theoretically because it is a linear system as far as the subthreshold activity is concerned.

IV. DISCUSSION

The use of noise with a certain degree of correlation improves ASR performance in the sense that a lower noise amplitude is required to optimize the input-output fidelity. This effect is explained by the quasistatic assumption; i.e., noise with a certain level of correlation is more efficient than white noise to linearize the input-output function of the FHN. This result is in contrast with simulations done with a weakly periodically modulated bistable system with a double-well potential, where the correlation of the noise has been shown to impair SR [11].

The question of why a certain level of correlation in the added noise can improve ASR is then translated to why the correlated noise is more effective to linearize the input-output function of the neuron. In this work we provide some preliminary insights to the answer of this question. The key result is that the SFHN system can reproduce qualitatively the evolution of (σ^*) for different levels of correlation of the noise. This means that an interaction between the noise correlation time and the intrinsic subthreshold dynamics of the model [14] driven in the focus regime, which is similar for FHN and SFHN, may be at the basis of this phenomenon. Most of the values of the signal $S(t)$ are in the range where the system behaves as a focus. In the focus the membrane responds to a transient perturbation with a damped oscillation of v, and displays the property of resonance, i.e., some particular frequency contained in the input noise can be more amplified than others in the output v. This led us to the hypothesis that the noise with a value of λ_1 that better fits the resonance frequency of the system should be the more effective to linearize the input-output function, because it can be more amplified due to the resonance effect. Thus, the σ^* that maximizes the slope of the constant current intensity versus mean firing rate should be smaller.

Interestingly, such a phenomenon whereby the interplay of noise correlation time and deterministic resonance influences the behavior of the system has been reported in the case of a discrete-time dynamical system near a Hopf bifurcation in the presence of correlated multiplicative noise [15]. This study shows that the output coherence is optimized for the noise correlation time for which the frequency is as similar as possible to the deterministic frequency. Nevertheless, in the conditions of the present simulations, other factors that add complexity to this simple interpretation must be taken into account. The two lowest values of A were in the node regime. Moreover, the lower values of A within the focus produce only a very little resonance effect. The damping factor ζ of the linear system derived from Eq. (3.1) was between 0 and $1/\sqrt{2}$. This condition was satisfied only in the case of the three larger values of A. Thus, roughly speaking, only the upper half of the signal produced a resonance effect. In this situation, the changes in the ''effective resonance frequency'' of the system and its relation with the input-output fidelity are nontrivial. For the above-mentioned three larger values of A, the resonance frequency of our model ranges from 1.6 to 2.25. The more effective noise in the simulations was in the range from $\lambda_1 = 20$ to $\lambda_1 = 5$. Further studies, including simulations with a systematic change of the parameter of the model that determine the resonance frequency, i.e., τ, as well as simulations using other neuron models, are necessary to clarify this point. We will address these issues in future studies.

In conclusion, we examined the response of the FHN to a slow subthreshold aperiodic signal in the presence of noise. We showed that for each noise correlation, the system displayed ASR, in the sense that there was an intermediate noise amplitude that maximized the input-output covariance or the input-output correlation. Then, we investigated the influence of the noise correlation time on the ASR characteristics, that is, the optimal noise amplitude σ^* leading to ASR, and the corresponding level of the covariance C_0^*. We observed that σ^* first decreased with the noise correlation time, before increasing again, while C_0^* remained almost constant at first, before decaying. These results suggest that, in this system, noise of appropriate correlation time can enhance ASR. At this correlation level the effect of linearization of the input-output function of the FHN is more effective, and for this reason the required noise level σ^* is decreased. This increased efficiency in the linearization of the input-output function may be related to resonance phenomena between the intrinsic subthreshold dynamics of the model and the noise, but further studies are needed to test this hypothesis.

ACKNOWLEDGMENTS

One of the authors (A.C.) gratefully acknowledges the financial support from the Japan Society for the Promotion of Science (JSPS), and the hospitality and constant help of the staff and the students of the Division of Biophysical Engineering of Osaka University. A.C. also acknowledges the financial support from PEDECIBA (Uruguay).

[1] J. P. Segundo *et al.*, in *Origins: Brain and Self Organization*, edited by K. Pribram (Lawrence Erlbaum Associates, Hillsdale, NJ, 1994).
[2] K. Douglass *et al.*, Nature (London) **365**, 337 (1993).
[3] H. Spekreijse and H. Oosting, Kybernetik **7**, 22 (1970).
[4] A. Longtin, A. Bulsara, and F. Moss, Phys. Rev. Lett. **67**, 656 (1991); D. R. Chialvo and A. V. Apkarian, J. Stat. Phys. **70**, 375 (1993); A. Longtin, *ibid.* **70**, 309 (1993); X. Pei , K. Bachman, and F. Moss, Phys. Lett. A **206**, 61 (1995); H. E. Plesser and S. Tanaka, *ibid.* **225**, 228 (1997); A. R. Bulsara *et al.*, Phys. Rev. E **53**, 3958 (1996); M. Stemmler, Network **7**, 687 (1996).
[5] J. J. Collins, C. C. Carson, and T. T. Imhoff, Nature (London) **376**, 236 (1995).
[6] J. E. Levin and J. P. Miller, Nature (London) **380**, 165 (1996); J. J. Collins, T. T. Imhoff, and P. Grigg, J. Neurophysiol. **76**, 642 (1996).
[7] J. J. Collins, C. C. Chow, and T. T. Imhoff, Phys. Rev. E **52**, 3321 (1995); J. J. Collins *et al.*, *ibid.* **54**, 5575 (1996).
[8] D. R. Chialvo, A. Longtin, and J. Müller-Gerking, Phys. Rev. E **55**, 1798 (1997).
[9] A. Neiman, L. Schimansky-Geier, and F. Moss, Phys. Rev. E **56**, 9 (1997).
[10] F. Moss, D. Pierson, and D. O'Gorman, Int. J. Bifurcation Chaos Appl. Sci. Eng. **4**, 1383 (1994); A. Bulsara and L. Gammaitoni, Phys. Today **49** (3), 39 (1996).
[11] L. Gammaitoni *et al.*, Rev. Mod. Phys. **70**, 223 (1998).
[12] The half-width of the Hanning window was chosen so as to maximize C_1 for the conditions of the present simulation. However, the particular choice of this value has no incidence on the results. To avoid distortions in the estimation due to border effects, segments of length equal to the half-width of the Hanning window at the beginning and the end of the time series of $S(t)$ and $R(t)$ were not taken into account for computing C_0 and C_1.
[13] This method produced an estimate of the discharge rate that agreed well with $\overline{R(t)}$ obtained through the convolution of the pulse train with the Hanning window.
[14] D. Nozaki and Y. Yamamoto (unpublished).
[15] J. L. Cabrera and F. J. de la Rubia, Europhys. Lett. **39**, 123 (1997).